CYCLIC PLANE STRAIN COMPRESSION TESTS ON CEMENT TREATED SAND

Regina SALAS MONGE[1], Junichi KOSEKI[2] and Takeshi SATO[3]

ABSTRACT: A new plane strain compression testing system suitable for shearing stiff geomaterials and observing shear band formation was developed, and a series of both monotonic and cyclic PSC tests were conducted on rectangular prismatic specimens of cement-treated sand. Comparisons were made between monotonic and cyclic plane strain compression tests to evaluate the differences on the peak strength of specimens with and without a cyclic loading history. No evidence of a reduction in the peak strength of specimens subjected to large amplitude cyclic loading was found. To study strain localisation characteristics and their relation with the failure mechanism of cement-treated sand, maximum shear strain distributions were calculated based on digital photographs taken at different stages of loading during each test. Several significant observations on the characteristics of strain localisation could be made from these data.

Key Words: Strain localisation, cement-treated sand, residual deformation, peak strength, large amplitude cyclic loading, plane strain compression tests.

INTRODUCTION

In recent years, stiff geomaterials such as sedimentary soft rocks and cement treated soils have been used as part of important large scale engineering structures. However, despite having similar strength and deformation characteristics sedimentary soft rocks are employed for supporting critical structures such as bridge foundations while cement treated soils have been limited to secondary structures such as road bases and artificial fill islands. During the 1995 Hyogoken-Nambu earthquake, the Akashi Strait Bridge of which one abutment and one pier are standing on a sedimentary soft rock deposit, suffered no structural damage and exhibited minimal residual displacements of anchorages and piers (Yamagata et al. 1996), despite the fact that this earthquake was much more severe than the design earthquake motion. This fact suggests that the design procedures employed were overly conservative. On the other hand, in the performance-based design that has been introduced recently, residual deformations under large earthquake loads need to be properly estimated in order to guarantee secure but cost-effective structures. The effect of large amplitude cyclic loading on the strength and deformation properties of stiff geomaterials are not well understood, since the experimental study on this issue for this type of materials is scarce. Particularly, the effects of shear band formation on the accumulation of residual strains during cyclic loading are not yet clear.

Koseki et al. (2002) conducted large amplitude cyclic triaxial compression tests to study the deformation properties of two types of soft rocks as was reported in this same bulletin. The results suggested that shear band formation influences the rate of strain accumulation under large earthquake loading although the exact moment of formation of the shear band could not be discerned clearly due to the fact that in triaxial tests visual observation of the membrane-covered specimen through the water-filled cell is difficult.

[1] Formerly graduate student, Department of Civil Engineering, University of Tokyo
[2] Associate Professor, Institute of Industrial Science, University of Tokyo
[3] Research Associate, Institute of Industrial Science, University of Tokyo

In view of the above, a new plane strain compression (PSC) testing system suitable for shearing stiff geomaterials and observing shear band formation was developed, and a series of both monotonic and cyclic PSC tests were conducted on rectangular prismatic specimens of cement-treated sand to evaluate the influence of cyclic loading history on the specimen strength and shear band formation characteristics.

TESTING EQUIPMENT, MATERIAL AND METHODOLOGY

The material being tested is a cement-mixed sand prepared in laboratory with the composition shown in **Table 1**. The specimens used were 16cm high, 8cm long in the σ_2 direction and 6cm long in σ_3 direction (**Figure 1**). The specimens were compacted by tamping, and the number of drops was increased with each layer to ensure homogeneity. They were cured under water for 72 hours before unmolding, and the unmolded specimens were kept again under water until setup in the triaxial cell. The material showed a compressive strength of about 1960kPa (20kg/cm^2) in triaxial compression tests at a confining stress of 98kPa after an approximate total curing time of 168 hours (7 days).

Table 1. Mixing proportions and materials used for manufacturing the cement treated sand. (After Mihira and Koseki, 2001)

Material	Weight (%)
Dry Toyoura sand	66.3
Portland cement	10
Bentonite	5
Distilled water	18.7

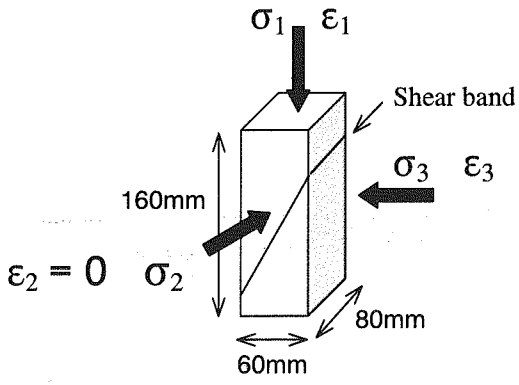

Figure 1. Rectangular prismatic specimens and stress state

The apparatus employed is a modified version, for conducting plane strain tests on a rectangular prismatic specimen, of the true triaxial testing system used by Hayano et al. (2001). It consists of a triaxial cell with a cell pressure capacity of 3MPa, a local measurement system for vertical and horizontal strains, a high precision hydraulic axial loading system and a data acquisition system.

For performing PSC tests a lateral restraining system, as shown in **Figure 2**, was used. The lateral load is measured by a load cell (LC2), attached between one of the confining platens and the end plate. The other confining plate is made of well polished transparent plexiglass which allows the deformation of the specimen's face to be observed accurately. To make the restraining system rigid enough for use with stiff geomaterials such as cement treated sand, the 3cm-thick transparent

plexiglass plate is attached to a 3cm-thick stiffening stainless steel frame which in turn is connected to an end plate by four stainless steel tie rods. To ensure smooth lateral displacement of the confining plates, both the stiffening frame and the end plate are supported by four small sliding rollers, which are sitting on the base of the triaxial cell. Friction force was measured by two additional load cells and vertical stresses were corrected accordingly. Additionally, to allow the movement in σ_3 direction that is necessary for free development of a single shear band with a plane parallel to σ_2 direction, the pedestal is mounted on a moving plate which in turn is lying on a set of two ball bearings which allow movement in σ_3 direction. For this same purpose, a thin silicon grease lubrication layer was applied at all rigid boundaries, that is at the interfaces of both the top cap and pedestal and the specimen and between the specimen and the confining plates.

All principal strains were measured locally to avoid effects of bedding error. As shown in **Figure 2**, axial strains ε_1 were measured using two vertical local deformation transducers (LDTs) placed vertically on opposite sides of the specimen. Lateral ε_2 strains in the restrained σ_2 direction were measured using six LDTs placed horizontally on the σ_3 surfaces, three on each side at different heights, and lateral ε_3 strains were measured using two pairs of proximeters and aluminum foil targets attached at two different heights on the σ_3 surfaces. Additionally, one, and in some tests two, external displacement transducers were placed on opposite sides outside the triaxial cell to measure axial strains for reference.

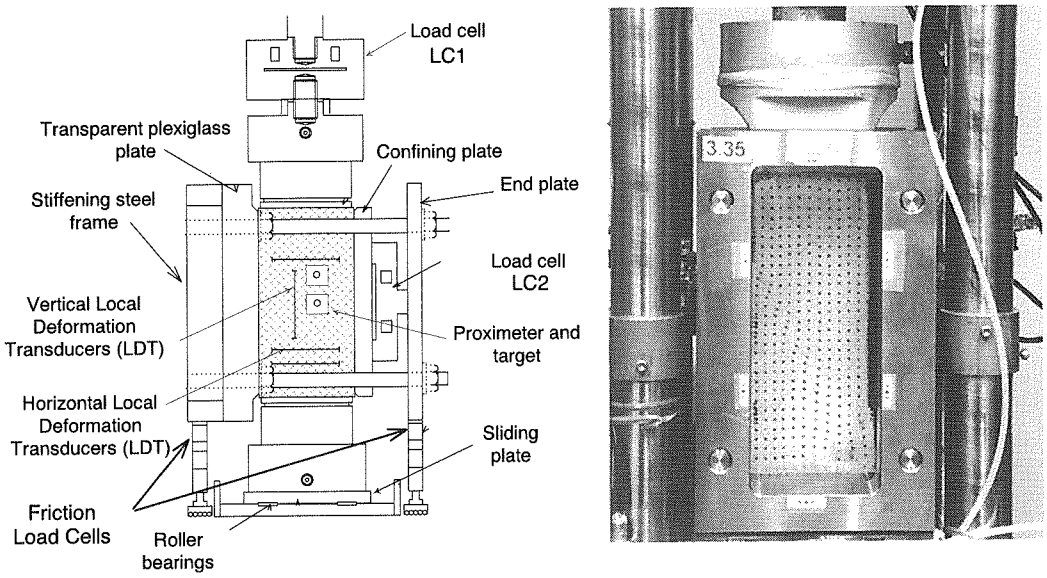

Figure 2. Lateral and front views of the plane strain compression (PSC) testing apparatus.

Each specimen was trimmed and set on the triaxial cell. It was saturated by a combination of vacuuming and back pressurizing to 196kPa (2kg/cm^2) in the triaxial cell filled with water (Ampadu and Tatsuoka 1993). To facilitate drainage a side drain of filter paper was used. The specimen was then isotropically consolidated up to a confining stress of 49kPa (0.5kg/cm^2) and left overnight for stabilization. After consolidation, the cell pressure and backpressure were decreased simultaneously and substituted by vacuum to keep the specimen under an isotropic stress condition. After removing the triaxial cell, the lateral restraining system was installed, and an initial deviator stress ($q_{2o}= \sigma_2-\sigma_3$) was applied in the σ_2 direction to ensure good contact between the confining plates and the specimen.

Specimens were then sheared under undrained condition. Both monotonic and cyclic plane strain compression tests were performed. For cyclic tests, the effective vertical stress σ_1 was increased up to an initial deviator stress ($q_o = \sigma_{1o}-\sigma_{3o}$), which was set to about 50% of the peak deviator stress observed in the monotonic tests. Then, cyclic axial loading was performed for a predefined number of cycles (N_c) and with a constant double amplitude of cyclic deviator stress (q_d). Finally, the axial load was monotonically increased until the peak deviator stress (q_{max}) was reached and then until residual state was achieved. A typical cyclic test result and other test parameters are shown in **Figure 3**.

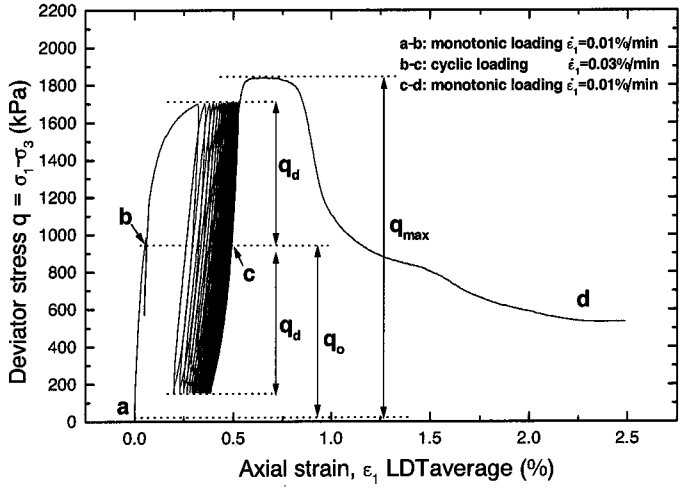

Figure 3. Typical stress strain relationship for the cyclic PSC tests and definition of stress parameters (Test PSCy02).

To study strain localisation characteristics and their relation with the failure mechanism of cement-treated sand, maximum shear strain ($\gamma_{max}=\varepsilon_1-\varepsilon_3$) and volumetric strain ($\varepsilon_{vol}=\varepsilon_1-\varepsilon_3$) distributions were calculated at different stages of loading. The new apparatus being used allows digital photographs of the specimen's σ_2 face to be taken through the transparent plexiglass plate and the membrane used had been imprinted with a series of points equally spaced every 5 mm (**Figure 2**). The horizontal and vertical displacements of each point were read from the photographs taken at different stages during the test. From this data the deformation at the center of each of the rectangular elements defined by the grid of points was calculated. Finally, strain fields showing the strain throughout the specimen's face at each of the stages of loading were plotted.

TEST RESULTS AND DISCUSSION

Six cyclic plane strain compression tests for different cyclic deviator stress q_d values and different number of cycles, as well as six monotonic plane strain compression tests were performed on cement treated sand specimens. The results obtained are presented herein.

Strain localisation characteristics of cement treated sand

From the strain fields calculated for the monotonic tests, it was observed that strain accumulation had different characteristics according to the phase in the stress-strain curve where it occurred. Three distinct behaviors were identified for the pre-peak, peak, and post-peak strain softening and residual states.

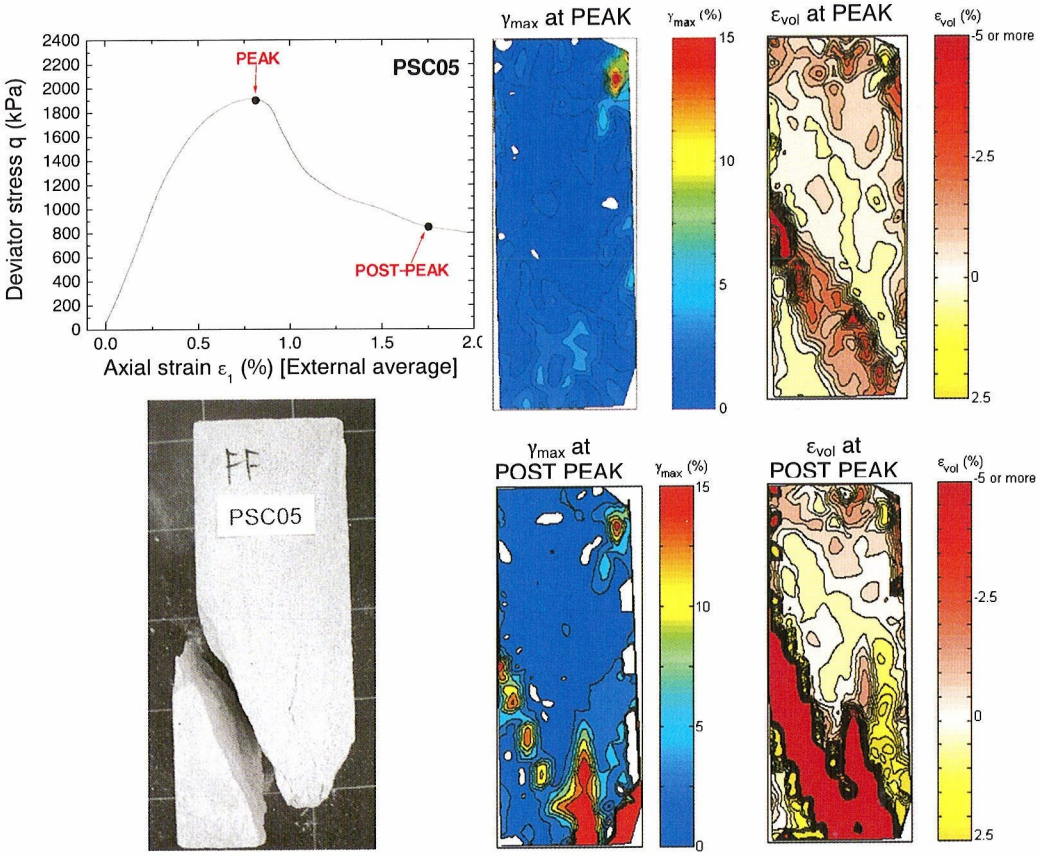

Figure 4. Strain localisation at peak and residual stress states for specimen PSC05 subjected to monotonic loading.

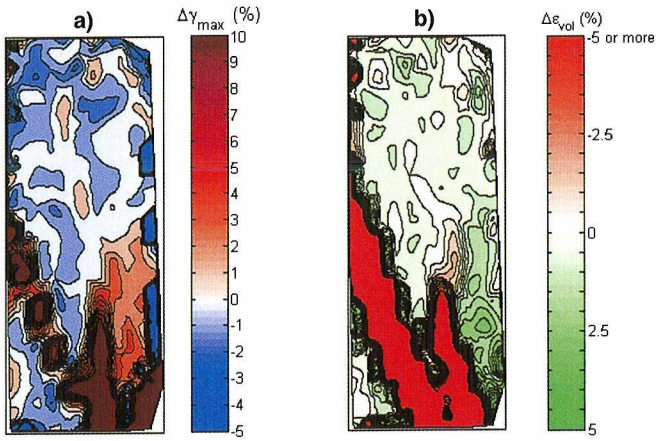

Figure 5. Increments of a)maximum shear strain $\Delta\gamma_{max}$ and b)volumetric strain $\Delta\varepsilon_{vol}$ accumulated during the post-peak strain softening drop for test PSC05.

During prepeak phase, deformation is quite uniform and no evident strain localisation seems to have taken place yet. As the stress level approaches peak stress state, strain starts to accumulate at different defined regions within the specimen, and several "candidate" shear bands start to appear simultaneously. After peak but while the peak stress level is sustained, accumulation continues to take place in all of these prospective shear bands but is very low or null outside these regions. Finally, during the post-peak drop, strain accumulation is limited to one (or two in some tests) of the "candidate" shear bands and continues until it is fully developed during residual state. **Figure 4** shows the maximum shear strain ($\gamma_{max}=\varepsilon_1-\varepsilon_3$) and volumetric strain ($\varepsilon_{vol}=\varepsilon_1-\varepsilon_3$) fields for the peak stress state and for a post-peak stress state for monotonic test PSC05. As may be observed, at peak stress state, γ_{max} accumulation is taking place simultaneously at several regions within the specimen and three "candidate" shear bands one in the upper right and two in the lower portion of specimen PSC05 are observed. However, during the post-peak stress drop only the two shear bands in the bottom portion fully developed. The strain distribution of the maximum shear strain increment $\Delta\gamma_{max}$ during the post peak stress drop (**Figure 5**) illustrates how the strain accumulation was restricted almost completely to those shear bands that later fully developed. The zones outside these shear bands not only stopped accumulating strain but also experienced a certain degree of elastic rebound (negative $\Delta\gamma_{max}$ on the order of 1%). This strain recovery phenomenon and the strain localisation in the shear band zone could also be observed by comparing the local measurements of axial strain ε_1 made by vertical LDTs located across and outside the shear band and of lateral strain ε_3 measured in zones inside and outside the shear band by pairs of proximeters transducers as is shown in **Figure 6**.

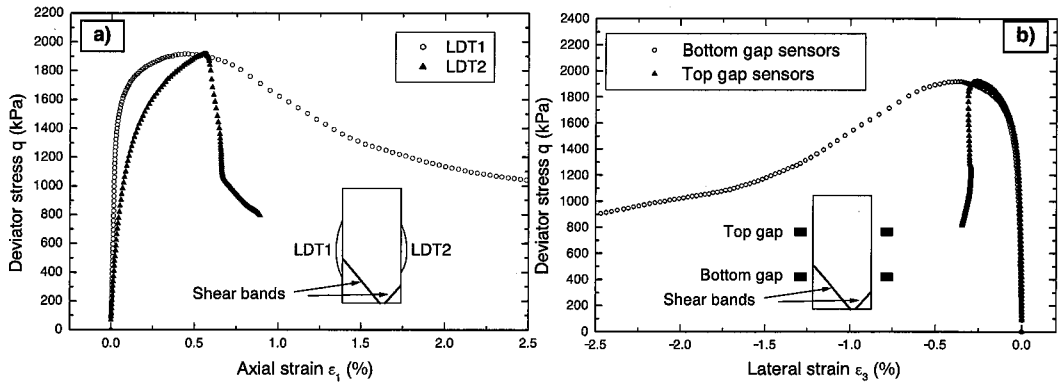

Figure 6. Relationships between deviator stress and a) axial strain ε_1 and b) lateral strain ε_3 for test PSC05.

In all tests, failure occurred when a certain threshold maximum shear strain value of around 10-15% was attained somewhere in the specimen. The value itself depends on grid size but qualitatively the fact remains that a similar γ_{max} value was mobilized at peak stress state for all specimens whether they had been subjected to cyclic loading previously or not. In the case of specimen PSC05 the threshold γ_{max} was attained in the candidate shear band in the upper right corner (**Figure 4**) even though this was not the shear band that fully developed later on. In some tests the shear band that continued dilating (fully developed) was not yet fully identifiable in the strain distribution at peak stress state and did not appear completely until the strain-softening regime (post-peak stress drop). All specimens, subjected to cyclic loading or not, could be easily separated after the test along the planes of the shear bands that fully developed and cracks were visible at the regions in the "candidate" shear bands where γ_{max} had reached around 15% but for which dilation and accumulation stopped (i.e. strain localisation regions that did not develop into full fledged shear bands). Refer to **Figure 4** and **Figure 7** for examples.

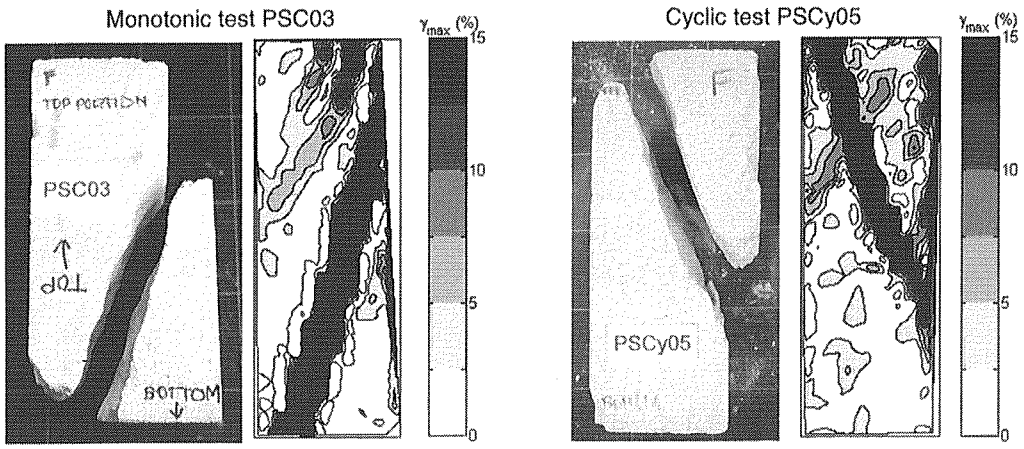

Figure 7. Specimens PSC03 and PSCy05 after testing and respective γ_{max} distributions at residual state.

Residual axial strain accumulation during cyclic loading

The accumulated axial strains ε_r measured at a same stress level of $q=q_o$ after each cycle, which include those accumulated during the initial monotonic loading, are plotted versus the number of cycles in **Figure 8** for each of the cyclic tests. The ε_r values shown were calculated from the average of the measurements of both vertical LDTs. The dotted line corresponds to the lowest axial strain measured by vertical LDTs, at which failure occurred among the monotonic tests and has been included as reference. In general, accumulation of residual strain during the cyclic loading was gradual and also to a limited extent. Most of the strain was accumulated during the first cycle, which corresponds to the initial virgin loading and after the first 10 cycles or so the residual axial strain increments per cycle become almost negligible. It must be noted that the strain accumulated during the first cycle differed among the different tests.

During the cyclic loading stage, the accumulated residual strain for all the cyclic tests except one was below the reference axial strain at peak $(\varepsilon_1)_{peak}$ observed in monotonic tests. It was determined from the γ_{max} strain fields that in test PSCy04, the only one that exceeded this threshold strain, a shear band formed and completely developed during the cyclic loading. This was also the only specimen which failed during the cyclic loading. In the remaining tests a limited amount of strain localisation took place during cyclic loading but no shear bands fully formed.

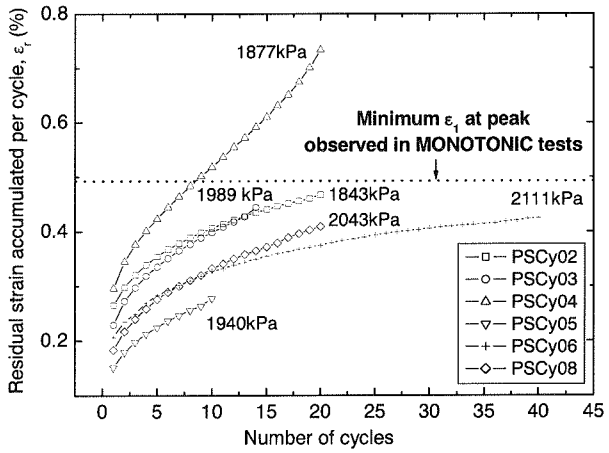

Figure 8. Accumulated residual strains ε_r measured at $q=q_o$ after each cycle. The measurement corresponds to the average of LDTs and the labels to peak deviator stress q_{max} values.

Strain distributions at different stages for test PSCy04 as well as the stress-strain relationships measured by each of the vertical LDTs are shown in **Figure 9**. As can be observed, the specimen failed during cyclic loading. It was determined from the data that the peak strength q_{max} was mobilized during the 11th cycle and had a value of 1877kPa, slightly higher than the average maximum stress q_o+q_d of 1863kPa that was being applied during the cyclic loading. Despite having failed, the cyclic deviator stress being applied could be sustained until the 20 cycles of loading were completed. During the test, it was not possible to determine that the peak strength had already been reached and thus the stress path was followed as planned. After the last cycle was completed the strain rate was reduced to the value used for monotonic portions which was one third of that used for the cyclic loading, and the deviator stress was increased monotonically. During this final monotonic loading stage, the higher deviator stress q that could be reached was 1820kPa (about 97%q_{max}). The reason behind the ability of the specimen to withstand a stress practically equal to q_{max} for such a large number of cycles after failure might be the faster strain rate that was being employed. However, in this research the effects of strain rate were not considered and the issue should be studied further.

In agreement with the strain localisation characteristics observed for the other tests, after 10 cycles a maximum shear strain of 15% had been mobilized at two different regions within specimen PSCy04 and also a residual axial strain ε_r of 0.5% which was the average axial strain at failure for the monotonic tests had already been accumulated (**Figure 9**). At this point two "candidate" shear bands started to appear: one in the upper central part and another in the right side of the specimen at middle height and within the area crossed by LDT2. After 15 cycles, the shear band in the upper part of the specimen had already appeared completely in the γ_{max} strain distributions and was dilating. The differences in the strain recorded by both LDTs were visible since the beginning. During the first cycles LDT2, which did not cross the region where the fully developed shear band appeared, presented more accumulation. The reason for this was that during the first 5 cycles more strain localisation took place in the region of the "potential" shear band located at the right side and that later did not develop further. On the other hand, during the final 3 or 4 cycles of the cyclic loading more accumulation was measured by LDT1 (which did cross the shear band that fully developed) and it continued all through the strain-softening regime while LDT2 stopped accumulating strain during the post-peak drop.

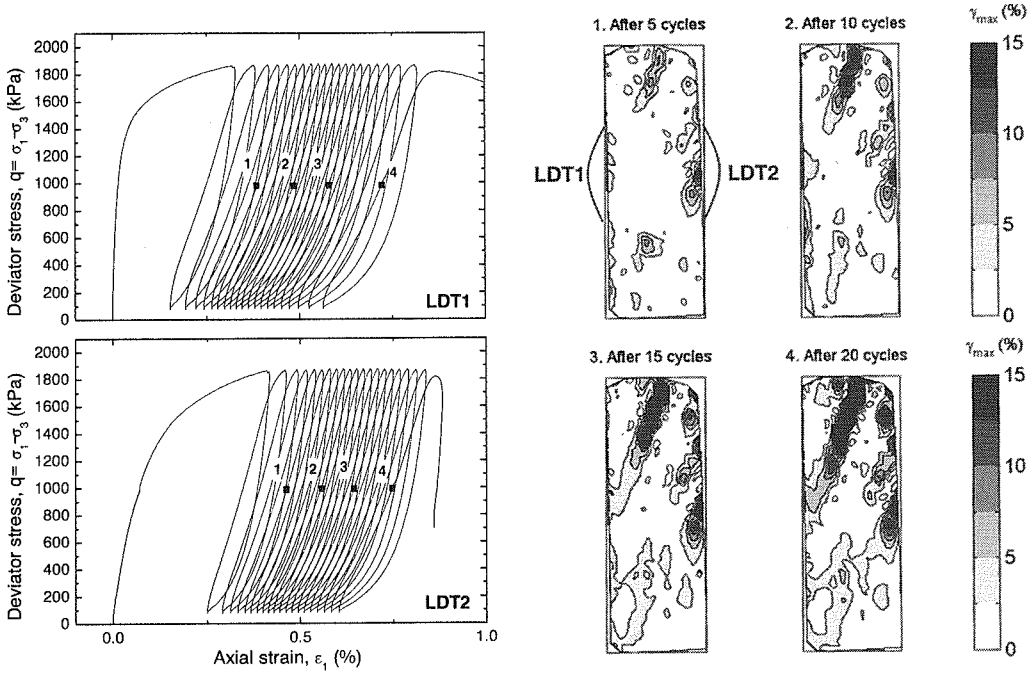

Figure 9. Strain localisation during cyclic loading in specimen PSCy04.

The same residual strains per cycle shown previously in **Figure 8** were normalized by the residual strain accumulated after the 1st cycle in order to compare the rate of strain accumulation between different tests and plotted in **Figure 10**. The rate of accumulation of ε_r seems to be similar for all the tests that had the same amplitude of cyclic shear strain. The rate at which ε_r accumulated was much slower for Test PSCy02 to which a smaller amplitude of cyclic loading q_d was applied. This suggests that the rate of strain accumulation increases with the q_d value. The same behavior has previously been observed for sedimentary soft rock (Koseki et al. 2002).

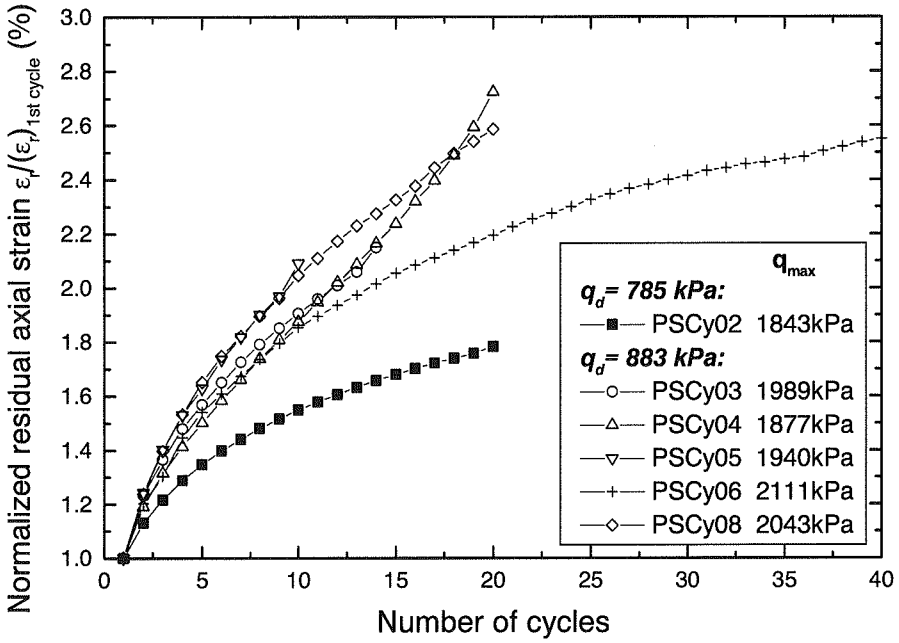

Figure 10. Rate of residual strain accumulation during cyclic loading.

Koseki et al. (2002) suggested that formation of a shear band during cyclic loading would be reflected as a sudden increase in the rate of ε_r accumulation. However, in the triaxial tests they performed the exact moment when the shear band formed could not be observed. In the current series of tests, specimen PSCy04 (20 cycles) showed a clear increase in the rate of residual strain accumulation after approximately 10 cycles. This is exactly the moment in which it was determined from the strain distributions that a shear band had formed. Another test, PSCy03, showed a subtler increase in the rate of accumulation of ε_r but only for the two or three last cycles (**Figure 10**). Although this specimen did not fail during the cyclic loading, the change in the rate of strain accumulation suggested that a shear band had started to form towards the end of the cyclic loading and this supposition was confirmed by the γ_{max} distributions. It is not known whether the specimen would have failed, as PSCy04 did, had the cyclic loading continued.

Peak strength of specimens subjected to cyclic loading history

All the tests, monotonic and cyclic, were performed for specimens with curing times of 176 ± 20 hours, except for two monotonic tests in which specimens with long curing times were used. The peak deviator stress q_{max} obtained for the tests with similar curing times (176 ± 20 hours) are plotted in **Figure 11**, together with data from one of the long curing time monotonic tests as reference (Test PSC04, curing time: 239 hours). Note that two of the monotonic tests in that figure were conducted with a smaller initial $q_{2o}= \sigma_2-\sigma_3$ value than the cyclic tests to which a q_{2o}= 50kPa was applied. It has been observed that q_{2o} may have an influence in the peak deviator stress values.

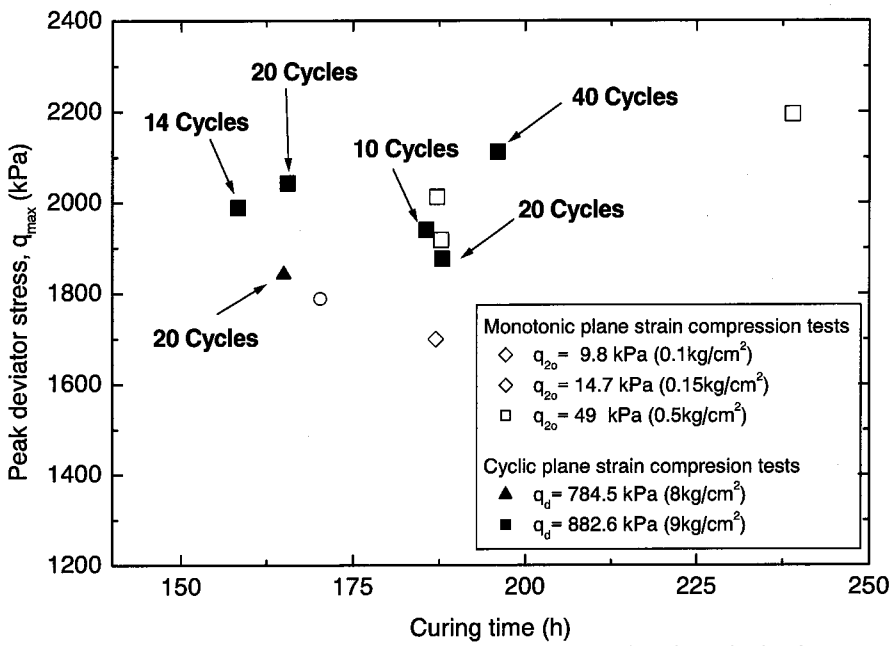

Figure 11. Maximum deviator stress in terms of curing time obtained for cyclic and monotonic PSC tests.

The variation of the maximum deviator stress is less than ±7% for the tests, monotonic and cyclic, conducted under the same initial q_{2o} condition. Although the test with "long" curing time did have a higher peak strength than the rest, it seems that the peak deviator stress values variation cannot be directly attributed to changes in curing time, at least for the limited range of the variations of curing times of the specimens used in this research. Additionally, as the figure shows, the scatter in the peak strength values is aleatory and no systematic difference of the peak strength between specimens subjected to cyclic loading and those that were not could be observed. Koseki et al.(2002) reported similar observations on sedimentary soft mudstone and a silty sandstone, the latter even showed an increase in the q_{max} value when subjected to a cyclic loading history.

CONCLUSIONS

The following conclusions can be drawn from the test results presented in this paper:

1. The deformation properties of cement treated sand under plane strain compression could be evaluated through the use of strain distributions calculated from photographs taken at different stages of loading during each test. The maximum shear strain distributions showed clearly and accurately the progressive accumulation of strain during the test and proved useful for observing shear band formation and determining the moment when the accumulation of strain ceases to be uniform and strain localisation starts taking place.
2. Different behaviors of strain localisation were identified for the pre-peak, peak, and post-peak states in cement treated sand specimens. During the pre-peak stage, deformation is quite uniform and no strain localisation seems to be occurring yet. As the stress level approaches peak stress state, several "candidate" shear bands or strain localisation regions begin to appear and develop simultaneously. During the post-peak strain-softening regime, strain accumulation is restricted almost completely to one or two shear bands that fully develop later on and the deformation in the remaining "candidate" shear bands seems to stop and evident rebound of the regions outside the shear bands that fully developed could be observed.

3. There seems to be a threshold value of maximum shear strain, intrinsic to the material, for which failure occurs. In addition to that, the axial strain at peak stress state measured with local deformation transducers was similar for all tests. It is reasonable to think that a certain failure envelope exists and that after surpassing a certain shear strain level and thus a related axial strain, failure occurs.
4. It was confirmed by comparing the residual axial strains accumulated per cycle and the respective γ_{max} distributions, that shear band formation usually manifests itself as a sudden change in the rate of residual strain accumulation during cyclic loading. The specimen that showed the lower peak strength failed during the cyclic loading and it was confirmed that a shear band appeared and developed during this period.
5. No evidence of a reduction in the peak strength of specimens of cement treated sand subjected to large amplitude cyclic loading with respect to the specimens sheared without a cyclic loading history was found.

ACKNOWLEDGEMENTS

The authors want to express deep gratitude to Mr. Shingo Mihira for the help provided regarding the procedure for preparing the cement treated sand specimens. A special acknowledgement to Mr. Kenji Watanabe of the Railway Technical Research Institute for the assistance he provided with the methodology for calculating the strain distributions. Special thanks to Prof. Ikuo Towhata for his valuable suggestions and interest in this research.

REFERENCES

Ampadu, S.K. and Tatsuoka, F. (1993). "Effects of setting method on the behavior of clays in triaxial compression from saturation to undrained shear." *Soils and Foundations*, JGS, No.33, Vol.2, 14-34.

Hayano, K. and Sato, T. (2001). "Development of true triaxial testing system to evaluate anisotropy of elastic characteristics on sedimentary soft rock." *Proceedings of the 15th International Conference on Soil Mechanics and Geotechnical Engineering*, A.A.Balkema Publishers, Vol. 1, 109-112.

Koseki, J., Indo, H., Hayano, K., Sato, T. and Torimitsu, M. (2002). "Cyclic triaxial tests on deformation properties of soft rocks." *Bulletin of ERS*, No. 35, 163-174.

Mihira, S. and Koseki, J. (2001). "Unconfined and Triaxial Tensile Tests on Cement Treated Sand." *Proc. of 56th Annual Conference of Japan Society of Civil Engineers*, 3-(A), pp.310-311 (in Japanese).

Yamagata, M., Yasuda, M., Nitta, A. and Yamamoto, S. (1996). "Effects on the Akashi Kaikyo Bridge." *Special Issue of Soils and Foundations on Geotechnical Aspects of the January 17 1995 Hyogoken-Nambu Earthquake*, Japanese Geotechnical Society, Vol. 1, 179-187.